Molecular Crystals and Liquid Crystals

Publication details, including instructions for authors and subscription information:
http://www.tandfonline.com/loi/gmcl20

Pyroelectric Thermowave Probing and Polarization Reversal in TGS/PEO Composites

Svetlana Bravina [a], Nicolas Morozovsky [a], Jan Kulek [b] & Bozena Hilczer [b]

[a] Institute of Physics of NASU, Kyiv, Ukraine

[b] Institute of Molecular Physics PAN, Poznan, Poland

Version of record first published: 10 Jun 2010

To cite this article: Svetlana Bravina, Nicolas Morozovsky, Jan Kulek & Bozena Hilczer (2008): Pyroelectric Thermowave Probing and Polarization Reversal in TGS/PEO Composites, Molecular Crystals and Liquid Crystals, 497:1, 109/[441]-120/[452]

To link to this article: http://dx.doi.org/10.1080/15421400802458761

Mol. Cryst. Liq. Cryst., Vol. 497, pp. 109/[441]–120/[452], 2008

ISSN: 1542-1406 print/1563-5287 online
DOI: 10.1080/15421400802458761

Pyroelectric Thermowave Probing and Polarization Reversal in TGS/PEO Composites

Svetlana Bravina[1], Nicolas Morozovsky[1], Jan Kulek[2], and Bozena Hilczer[2]
[1]Institute of Physics of NASU, Kyiv, Ukraine
[2]Institute of Molecular Physics PAN, Poznan, Poland

The pyroelectric response U_π *of triglycine sulphate/polyethylene oxide composites is investigated by the photothermomodulation method in the course of polarization reversal under the action of an external voltage* V. *The thermowave profiles derived from the dependence of* U_π *on the IR-flux modulation frequency indicate changes of the distribution of pyroelectric parameters over the thickness at different polarization reversal stages. The study of* U_π (V)*-loops shows a large start-finish voltage interval of the polarization reversal. Two phases in the polarization reversal that are distinguished by a difference in time scales in the polarization switching process are revealed. The thermowave probing proved to be an efficient tool for studying the polarization reversal in ferroelectric particles in multiphase matrices.*

Keywords: composites $TGS_{0.5}/PEO_{0.5}$; polarization reversal and switching; pyroelectric response

1. INTRODUCTION

Ferroelectric crystal – polymer composites are materials attractive both for fundamental and applied studies of electro-active properties of systems of confined ferroelectric particles with different degrees of interaction with matrices. The components of the composite under investigation, $TGS_{0.5}/PEO_{0.5}$, are a ferroelectric molecular crystal of triglycine sulphate (TGS), $(NH_2CH_2COOH)_3 \cdot H_2SO_4$, and a high-molecular-weight polymer poly(ethylene oxide) (PEO), $(\ldots -CH_2-O-CH_2-\ldots)_n$ $(n = 2 \cdot 10^5 – 4 \cdot 10^6)$.

TGS is well known as a water-soluble ferroelectric with the 180°-domain structure and remains, despite its hygroscopicity, the best

Address correspondence to Svetlana Bravina, Institute of Physics of NASU, 46, Prospect Nauki, Kyiv 03028, Ukraine. E-mail: bravmorozo@yahoo.com

material for highly sensitive pyroelectric detectors of radiation (PDR) [1–3]. Ferroelectric properties and high pyroelectric activity of TGS single crystalline thin layers and particles are conserved up to the μm scale [3–5].

PEO is a synthetic polymer used in the pure non-ionic state as a surfactant and as a water-soluble thermoplastic resin for thickening and other industrial applications. Dispersing salts at a sufficiently high molecular level allows the ionic transport under RT conditions and transforms PEO into a polymer-salt electrolyte which is used as an ionic conducting polymer for Li-batteries, displays, sensors, and other electrochemical devices [6–9].

$TGS_{0.5}/PEO_{0.5}$ hot-pressed composite exhibits the sufficient pyroelectric activity. Namely, the evaluated value of the pyroelectric coefficient γ for $TGS_{0.5}/PEO_{0.5}$ is $\approx 7 \cdot 10^{-5}\,C/m^2\,K$ [5]. It is higher than that for TGS/Si-rubber 60/40 composite, whose value is $1.6 \cdot 10^{-5}\,C/m^2\,K$ [4], and is in correspondence with random polar directions of TGS particles and the 50% part of TGS in these composites. Ferroelectric properties of $TGS_{0.5}/PEO_{0.5}$ composite, in particular the polarization reversal, have not been investigated despite the specific character expected for such a case of the composite components with the unique collection of properties interesting for science and practically important. The ferroelectric characterization of a multiphase structure related to the polarization distribution is of a special interest.

Earlier, we performed the study of details of polar inhomogeneities in PVDF-based structures [10] and examined the time scale peculiarities of the polarization reversal process in PZT-film/Si-substrate structures [11] by the photothermomodulation method [10,12]. The results obtained prove the efficiency of this method due to its possibility to elucidate peculiarities of the polar activity distribution transformed with time under an applied external voltage.

The paper presents the results of studying the peculiarities of the distributions of pyroelectric and dielectric parameters along the thickness of $TGS_{0.5}/PEO_{0.5}$ composite samples and the polarization reversal and switching by means of the photothermomodulation method.

2. EXPERIMENTAL

2.1. Samples

$TGS_{0.5}/PEO_{0.5}$ composites with 50/50 volumetric content were prepared by the hot pressing method at $T_{hp} \approx 70^{\circ}C$ at the uniaxial pressure $P_{hp} = 500\,MPa$ applied during $t_{hp} = 30\,min$. The samples were slowly cooled under the pressure to room temperature, at which the pressure was taken off.

TGS crystals were grown from an aqueous solution with stoichiometric pH value at $T > T_C = 49°C$. The material was purified by 5-fold recrystallization.

Polyethylene oxide (Aldrich) of an average molecular weight of $6 \cdot 10^5$ was mixed with a TGS powder with the average dimension of TGS particles around 5 μm and milled before the hot pressing.

The samples of 0.25–0.35 mm in thickness and 30–50 mm^2 in area were covered with Ag-electrodes.

The measurements were performed under an ambient humidity of $60 \pm 5\%$.

2.2. Measurements

For pyroelectric investigations, we applied the developed [1,3] and then modified [10,11] photothermomodulation method, in which the amplitude-frequency $U_\pi(f_m)$ and phase-frequency $\varphi_\pi(f_m)$ dependences of the pyroelectric response are investigated for the samples under the conditions of operation of a sensitive element (SE) of PDR in a wide modulation range of the frequency f_m. The measurements of the pyroelectric response U_π can be performed in the pyroelectric current mode, when $2\pi f_m r_l C_s < 1$ and $U_\pi = U_{\pi 1} \propto (\gamma/c_1) r_l$, and in the pyroelectric voltage mode, when $2\pi f_m r_l C_s > 1$ and $U_\pi = U_{\pi 2} \propto (\gamma/c_1 \varepsilon)/f_m$, where γ denotes the pyroelectric coefficient, c_1 is the volume thermal capacity, r_l is the load electrical resistance, and C_s is the capacitance of the sample. For dielectric samples, the measurements of $U_{\pi 1}$ and $U_{\pi 2}$ give the possibility to evaluate the effective dielectric permittivity ε_π from the dielectric ratio $D_\pi = U_{\pi 1}/U_{\pi 2} f_m \propto \varepsilon_\pi$.

The analysis of the $U_\pi(f_m)$ and $\varphi_\pi(f_m)$ characteristics (f_m-spectra) under sinusoidally modulated radiation flux due to the fundamental relationship between the f_m and the length of a temperature wave $\lambda_T = (a_T/\pi f_m)^{1/2}$ (a_T is the thermal diffusivity) gives the possibility to obtain the thermowave profiles $U_{\pi 1,2}(\lambda_T)$ (λ_T-profiles). So, the information about the undersurface distribution of effective pyroelectric figures of merit $M_1 = \gamma/c_1$ and $M_2 = \gamma/c_1 \varepsilon$ can be obtained.

Application of the external electrical voltage V allows the study of the $U_\pi(V)$ and $\varphi_\pi(V)$ dependences and the temporal variations of U_π and φ_π under $V = \text{const}$, in particular under the conditions of polarization reversal (under the external voltage cycling between positive and negative V values) and polarization switching (under changing a sign of the external dc voltage). Because $\varphi_{\pi 1,2}$ values are directly connected with the direction of the pyroelectric current ($\varphi_{\pi 1}$) or the sign of the pyroelectric charge ($\varphi_{\pi 2}$) and with the sign of the pyroelectric reaction, the result of the polarization reversal is clearly visible by the 180°-change of the $\varphi_{\pi 1,2}$ values.

3. RESULTS AND DISCUSSION

3.1. Pyroelectric Response – Modulation Frequency Characteristics

The f_m-spectra of $U_{\pi 1,2}$-, $U_{\pi 2} \cdot f_m$-, D_π- and $\varphi_{\pi 1,2}$-f_m-spectra obtained in a polarized state under different polarities of the poling voltage and in a depolarized state are presented in Figure 1a, b, and c.

For both polarities of the poling voltage, the shapes of f_m-spectra of $U_{\pi 1,2}$ and $U_{\pi 2} \cdot f_m$ obtained under pyroelectric excitation of (+)- and (−)- electrodes (being positive ≪+≫ and negative ≪−≫ under poling) are near symmetrical relatively to the low-f_m edge. The existence of the 180°-difference between $\varphi_{\pi 1,2}$ values on f_m-spectra of $\varphi_{\pi 1,2}$ obtained for the (+)- and (−)- electrodes corresponds to the different signs of the pyroelectric reaction for the opposite directions of the effective polarization P_{se} relative to the electrodes.

For the same sample in the polarized state and in the repolarized one (polarized under opposite V_{dc} polarity) (compare Fig. 1a and b), the reverse of a polarity of the poling voltage changes insignificantly the shape of f_m-spectra and in correspondence with the change of the sign of the pyroelectric reaction leads to the 180°-change of $\varphi_{\pi 1,2}$ values.

Depolarized samples (Fig. 1c) are characterized by a significant decrease of the $U_{\pi 1,2}$-response level. As a consequence, changes in the corresponding f_m-spectra and a decrease of $U_\pi \cdot f_m$ values followed by a variation in the D_π values are observed. The symmetrical shape of $\varphi_{\pi 1,2}$-f_m-spectra observed in the depolarized state (Fig. 1c) corresponds to the same $\varphi_{\pi 1,2}$ values and indicates the same sign of the pyroelectric reaction under the both electrodes and so the same P_{se} direction, relative to the electrodes. Indeed, the ≪+≫ sign of the pyroelectric reaction remains for one electrode (marked (o) in Fig. 1c), and also ≪+≫ instead of ≪−≫ appears on the other electrode (marked (x) in Fig. 1c) under the depoling process.

3.2. Pyroelectric Parameters – Thermo-Wave Profiles

The λ_T-profiles of M_1, M_2, and D_π obtained by the conventional treatment of the f_m-spectra under different polarities of the poling voltage (Figs. 1a, b, and c) are presented in Figure 2a, b, and c.

The estimation of the diffusivity α_T of $TGS_{0.5}/PEO_{0.5}$ composites necessary for the conversion of the f_m-spectra into λ_T-profiles was performed from the measurements of the phase shift of the pyroelectric response in the back geometry [13]. The obtained value $\alpha_T \approx 1.5 \cdot 10^{-7}\,m^2/s$ is close to that known for low-density polyethylene [14], $1.65 \cdot 10^{-7}\,m^2/s$.

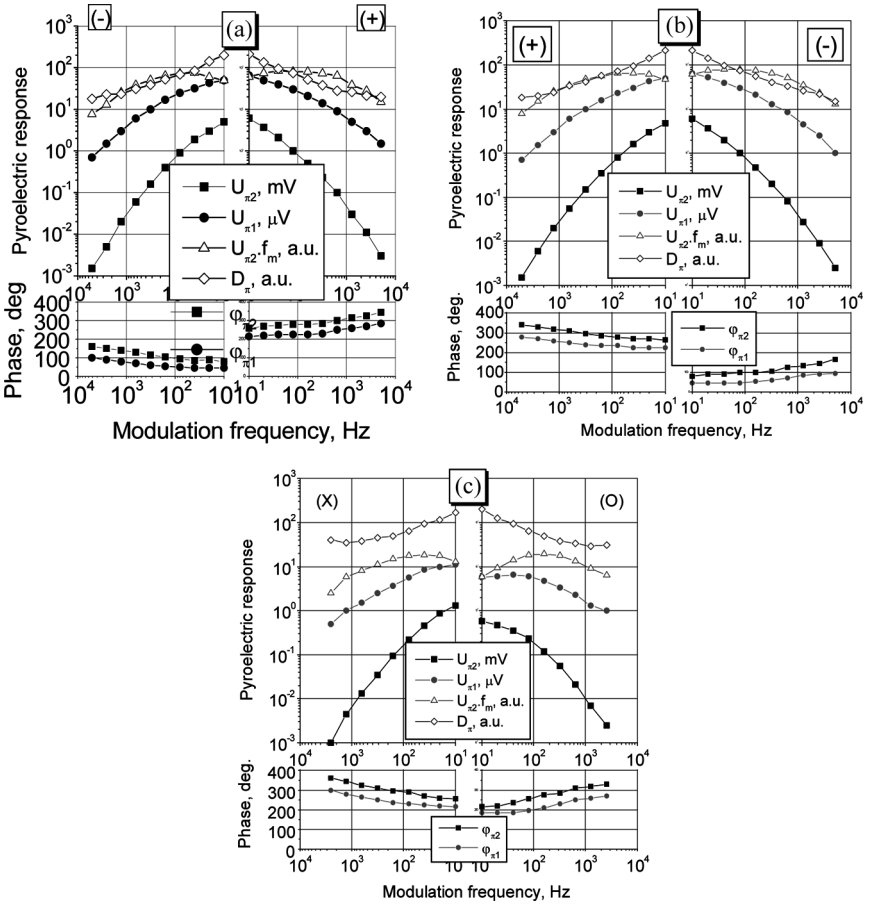

FIGURE 1 Modulation frequency spectra of the pyroelectric response for Ag-(TGS/PEO)-Ag: (a) unidirectionally poled state after the treatment with unipolar +10 V pulses at (o)-electrode; (b) reversed unidirectionally poled state after the treatment with unipolar +10 V pulses at (x)-electrode; (c) depolarized state after the time dosed treatment under alternative (+/−)10 V triangle voltage between (o)- and (x)- electrodes (marked).

For the same sample in the polarized and then repolarized states (compare Fig. 2a and 2b), the shapes of the corresponding λ_T-profiles and the values of $M_{1,2}$ and D_π are almost identical.

Inversion of $\varphi_{\pi 1,2}$-λ_T-profiles as a result of the repolarization (compare Fig. 1a and 1b) reflects a change of the P_{se} direction under both electrodes as a result of the polarization reversal.

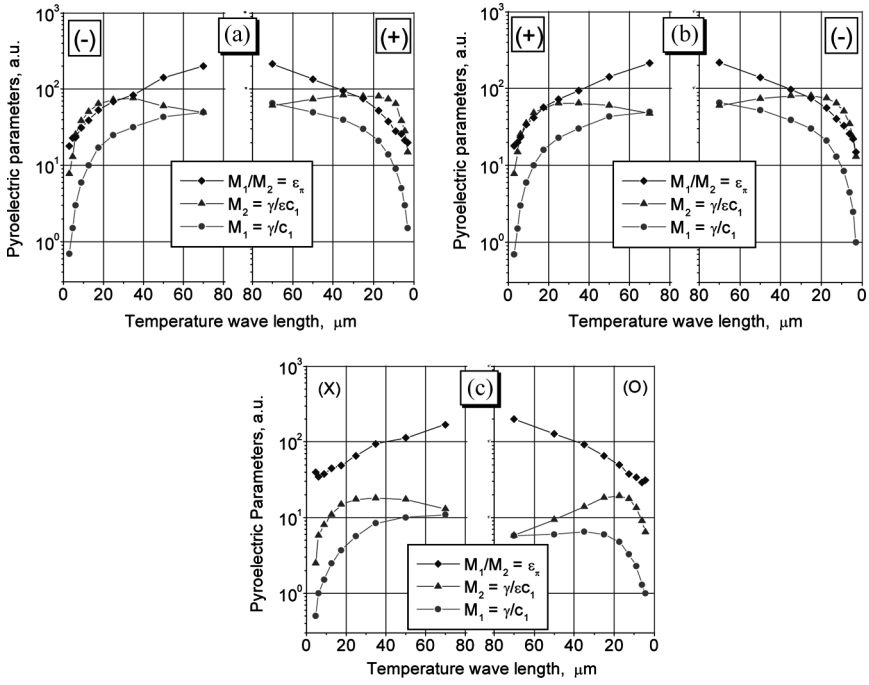

FIGURE 2 Thermowave profiles of the pyroelectric parameters for Ag-(TGS/PEO)-Ag. a, b, and c correspond to the same conditions as in Figure 1.

The symmetrical shape of $\varphi_{\pi 1,2}$-λ_T-profiles under excitation of both sides of the sample in a depolarized state (Fig. 1c) corresponds to the predominance of the same orientation of P_{se} in the regions near the both (o) and (x) electrodes. The same level of $\varphi_{\pi 1}$-λ_T-profiles, namely the same $\varphi_{\pi 1} = 180^\circ$ value for both (+)- and (−)- electrodes, indicates the formation of a state similar to the inversely polarized structure of the "head-to-head" type.

The results of the thermowave probing indicate the following peculiarities of the polar state in hot pressed $TGS_{0.5}/PEO_{0.5}$ composites:

1. significantly higher level of pyroactivity in volume than that in the near-surface region for the polarized state;
2. stronger change of a pyroactivity level in volume than in that in the near-surface region under transition from the polarized to depolarized state;
3. decay of λ_T-profiles of D_π and so of ε_π value from the volume to the surface for both the polarized and depolarized states.

The specificity of the observed λ_T-profiles can be related either to a higher concentration of TGS particles in volume than that in the under-surface layer of the composite with keeping the 0–3 type of connectivity or to a partial change in the connectivity from 0–3 to 1–3 type because of formating a partially continuous ferroelectric frame. Such a formation is considered as quite possible for composites with high concentration of ferroelectric particles under hot pressing [15].

3.3. Pyroelectric Response – External Voltage Polarization Reversal Characteristics

In contrast to TGS single crystals, the charge and current loops of the polarization reversal in $TGS_{0.5}/PEO_{0.5}$ composites are not observed up to the infra-low frequency range (Fig. 3a, b). However, changes in the f_m-spectra and λ_T-profiles induced by a variation of the external dc voltage sign clearly indicate the effect of polarization switching in the poling – depoling – repoling sequences (see Sections 3.1 and 3.2). These results agree with the possibility of polarization reversal under an arbitrarily low electric field of long enough duration, known for a number of ferroelectrics [16], in particular for $BaTiO_3$ [17,18].

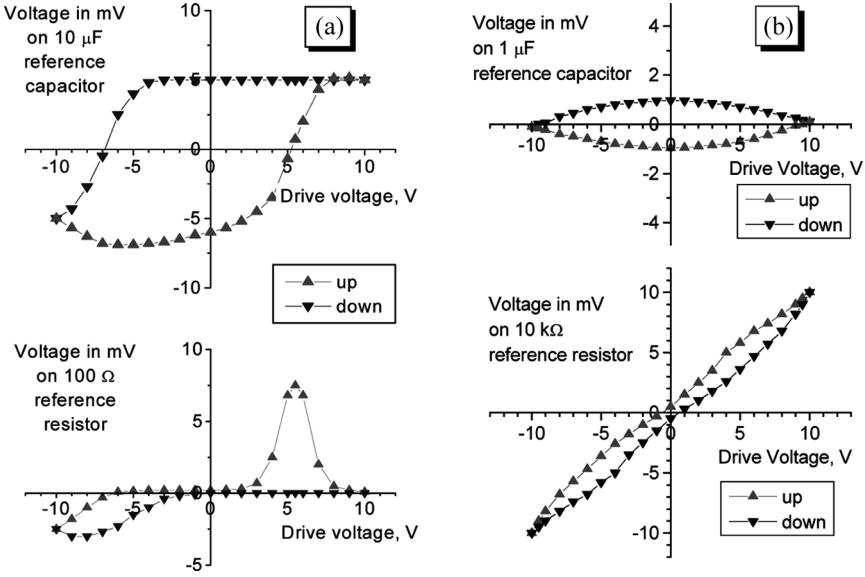

FIGURE 3 Charge-voltage (top) and current-voltage (bottom) polarization reversal loops under bipolar +/−10 V triangle pulses: (a) for Ag-TGS-Ag (0.2 mm thick TGS, water-ethanole damaged left side) at 40 Hz; (b) for Ag-TGS/PEO-Ag (0.35 mm thick $TGS_{0.5}/PEO_{0.5}$) at 0.1 Hz.

The examination of the polarization reversal was performed in the static mode at the step-change of V_{dc} ($\pm$(0.25–1) V) under its cycling between maximum positive and negative values.

The pyroelectric response-external voltage loops of the amplitude $|U_{\pi 1}|$ and phase $\varphi_{\pi 1}$ are presented in Figure 4. The $|U_{\pi 1}|$-V_{dc}-loops have a characteristic viaduct-like shape. The top edges of viaduct spans reflect the saturation of $|U_{\pi 1}|$ under an increase of V_{dc} in correspondence with the f_m-spectra in Figure 1a, b and the λ_T-profiles in Figure 2a, b. The sharp tips of viaduct pillars reflect the minimum $|U_{\pi 1}|$ value in the depolarized state and clearly indicate the coercive voltages $V_c^- \approx -4$ V and $V_c^+ \approx +5.5$ V. The f_m-spectra shown in Figure 1c and the λ_T-profiles in Figure 2c correspond to such depolarized state.

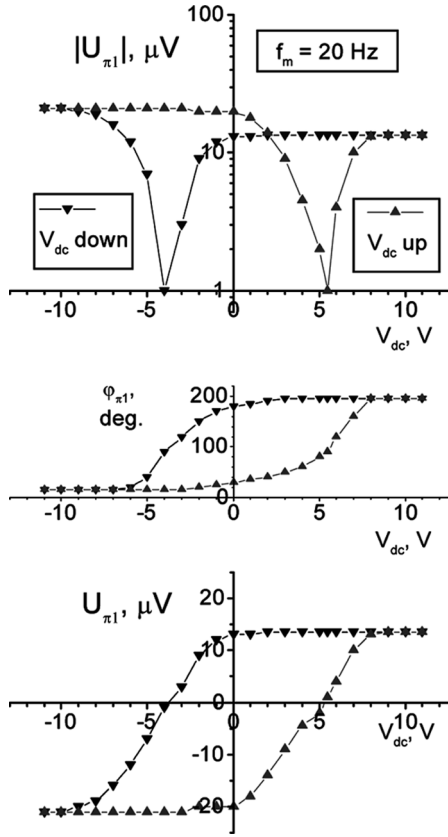

FIGURE 4 Pyroelectric response loops under the polarization reversal for Ag-TGS/PEO-Ag. Top: amplitude-voltage viaduct-like loop; Middle: phase-voltage loop; Bottom: reconstructed response-voltage parallelogram-like loop.

The asymmetry of the $|U_{\pi 1}(V_{dc})|$ viaduct spans indicates the difference in the final stages of polarization reversal processes considered as a difference of V_c^- and V_c^+ values. The asymmetry can be related to the sample technology (hot-pressing) that results in a unipolar behavior.

The asymmetry of the $|U_{\pi 1}(V_{dc})|$ viaduct pillars relative to $V_c^{\pm}$ indicates the appreciable distinction in decreasing the unipolarity degree at $|V_{dc}| < |V_c^{\pm}|$ and its increasing at $|V_{dc}| > |V_c^{\pm}|$. The values of "voltage rate" $d(\log U_{\pi 1})/dV_{dc}$ are near twice as much on the ascents of pillars than those on their inclines.

The shape of $\varphi_{\pi 1}(V_{dc})$-loops (Fig. 4) is in correspondence with the change of the sign of the pyroelectric reaction, which is related to the reverse of the P_{se} direction. The regions of $\pm 180^\circ$ $\varphi_{\pi 1}$-changes are in the vicinity of $V_c^{\pm}$ and $\varphi_\pi\,(V_{dc}) = \text{const}$ outside the range of $V_c^{\pm}$.

The reconstructed $U_{\pi 1}$-V_{dc}-loops obtained by combination of the amplitude $|U_{\pi 1}(V_{dc})|$ and the phase $\varphi_{\pi 1}(V_{dc})$ are presented in Figure 4.

The examination of the $U_{\pi 1}$-V-loops shows the complete saturation of $U_{\pi 1} \propto \gamma/c_1$, and the effective value $\gamma(V)$ for the both polarities of V_{dc}. The shape of $U_{\pi 1}$-V_{dc}-loops indicates the near linear dependence $U_{\pi 1}(V_{dc})$ in the large vicinity of the coercive voltages $V_c^{\pm}$. At that, the large voltage regions with decrease in the unipolarity degree at $|V_{dc}| < |V_c^{\pm}|$ and with increase in that at $|V_{dc}| > |V_c^{\pm}|$ with the noticeably differing "voltage rate" $dU_{\pi 1}(V_{dc})/dV_{dc}$ point out to the different phases of the polarization reversal process in the $|V_{dc}| < |V_c^{\pm}|$ and $|V_{dc}| > |V_c^{\pm}|$ regions, respectively.

The shape of $|U_{\pi 1}|$-V-loops reflects the variation of $\gamma = dP_{se}/dT$ during the polarization reversal process. In general, the obtained shape of $U_{\pi 1}$-V-loops is similar to that of the ferroelectric hysteresis loop (compare Fig. 4, bottom, and Fig. 3a as an example). As we obtain the complete saturation of the effective values $\gamma(V)$, we can consider the corresponding $P_{se}(V)$ as completely saturated.

One can observe that the coercive voltages for hot-pressed 0.35-mm-thick $TGS_{0.5}/PEO_{0.5}$ samples (Fig. 4) are near to those obtained for TGS samples of 0.2 mm in thickness (Fig. 3). This corresponds to the coercive field $E_c = 250 - 350$ V/cm which is close to E_c known for TGS at RT [18,19] and indicates that only a small part of the external voltage V_{dc} applied to a $TGS_{0.5}/PEO_{0.5}$ sample drops on the PEO interlayers.

3.4. Pyroelectric Response – External Voltage Polarization Switching Characteristics

The voltage dependences of saturated pyroelectric response amplitudes $|U_{\pi 1s}(V_{dc})|$, phases $\varphi_{\pi 1s}(V_{dc})$, and characteristic times $\tau_r(V_{dc})$

and $\tau_o(V_{dc})$ obtained in the polarization switching mode by changing the V_{dc} polarity are presented in Figure 5. The time $t = \tau_o$ corresponds to $U_{\pi 1}(t) = 0$ (pyroelectrically compensated state of TGS particles with partially reversed P_{se} directions similar to that obtained at $V_{dc} = V_c^{\pm}$, Fig. 4), whereas the time $t = \tau_r$ is characteristic of the saturated value $U_{\pi 1s}(V_{dc})$ that corresponds to the poled state with the maximum P_{se} at the coercive voltage V_{dc}.

Asymmetry of the positive ($V_{dc} > 0$) and negative ($V_{dc} < 0$) branches of the response amplitude $|U_{\pi 1s}(V_{dc})|$ corresponds to that obtained in the polarization reversal mode (see Fig. 4 and comments in Section 3.3). The 180°-differences in the phase angle $\varphi_{\pi s1}$ for the positive

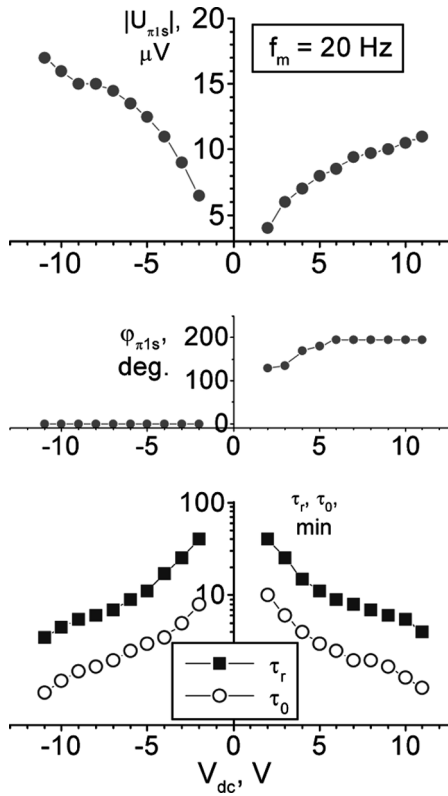

FIGURE 5 Saturated pyroelectric response in the course of polarization reversal for Ag-$TGS_{0.5}$/$PEO_{0.5}$-Ag. Top: saturated response amplitude; Middle: phase of saturated response; Bottom: characteristic times of polarization reversing τ_{rev} and zero-response τ_o.

and negative branches of $\varphi_{\pi 1s}(V_{dc})$ are in correspondence with different P_{se} directions under $V_{dc} > 0$ and $V_{dc} < 0$.

A large range of changes in $\tau_o(V_{dc})$ and $\tau_r(V_{dc})$ and their decrease show a strong external voltage dependence of the polarization switching rate and its strong acceleration under an increase in V_{dc} for $TGS_{0.5}/PEO_{0.5}$ composites.

The almost one-order difference in $\tau_o(V_{dc})$ and $\tau_r(V_{dc})$ (Fig. 5) reflects the difference in time scales of polarization switching in the voltage regions $|V_{dc}| < |V_c^{\pm}|$ and $|V_{dc}| > |V_c^{\pm}|$. This allows us to distinguish two phases of the polarization switching process in $TGS_{0.5}/PEO_{0.5}$ composites, namely the initial short-term phase at $t < \tau_o$ and the final long-term one at $\tau_o < t < \tau_r$.

The similar shape of the $\tau_o(V_{dc})$ and $\tau_r(V_{dc})$ dependences reflects the same peculiarities of P_{se} changing on both phases of the polarization switching.

CONCLUSIONS

1. The results of the thermowave probing of $TGS_{0.5}/PEO_{0.5}$ hot-pressed composites indicate the appreciable inhomogeneity of the λ_T-profiles over the sample thickness, which can be due either to a higher concentration of TGS particles in volume than that in the under-surface layer of $TGS_{0.5}/PEO_{0.5}$ composite or to the formation of a partially continuous ferroelectric framework in volume.
2. Sharp tails of the pyroelectric response amplitude, external voltage loops, distinctly determine the coercive voltage values. Due to the relationship between the $\varphi_{\pi 1,2}$ values and the sign of the pyroelectric reaction, the result of the polarization reversal is clearly visible in the 180°-change of the phases $\varphi_{\pi 1,2}$.
3. The analysis of peculiarities of the pyroelectric response–external voltage curves reveals two phases in the polarization reversal process with appreciably different "voltage rates," as well as in the polarization switching process distinguished by the time scale under applied voltages lower and higher than the coercive one.
4. The results of the thermowave probing, polarization reversal, and polarization switching demonstrate a possibility of tuning the pyroelectric parameters of $TGS_{0.5}/PEO_{0.5}$ hot-pressed composite by an externally applied voltage.
5. Pyroelectric response–external voltage loops can be considered as a thermal derivative analog of ferroelectric hysteresis loops.
6. The pyroelectric modulation method is an effective tool for studying the polarization reversal and switching in ferroelectric crystallites (grains) loaded in a polymer matrix.

REFERENCES

[1] Kremenchugsky, L. S. (1971). *Ferroelectric Detectors of Radiation*, Naukova Dumka: Kyiv (in Russian).
[2] Lang, S. B. (1974). *Sourcebook of Pyroelectricity*, Gordon and Breach: New York.
[3] Kremenchugsky, L. S. & Roitsina, O. V. (1979). *Pyroelectric Detectors of Radiation*, Naukova Dumka: Kyiv (in Russian).
[4] Mendiola, J., Jimenez, B., Alemany, C., & Maurer, E. (1981). *Ferroelectrics*, *39*, 1201.
[5] Kulek, J., Hilczer, B., Polomska, M., & Szczesniak, L. (1997). *Ferroelectrics*, *201*, 201.
[6] Wintersgill, M. C. & Fontanella, J. J. (1989). In: *Polymer electrolyte reviews-2*, MacCallum, J. R. & Vincent, C. A. (Eds.), Elsevier: London. Ch. 2, 41.
[7] Gray, F. M. (1997). *Polymer Electrolytes*, RSC Materials Monograph, The Royal Soc. of Chemistry: Cambridge.
[8] Wagner, A. & Kliem, H. (2002). *J. Appl. Phys.*, *91*(10), 6630.
[9] Saboormaleki, M., Barnes, A. R., & Schlindwein, W. S. Abstr. 726, 205-th Meeting, 2004, Electrochemical Society, Inc.
[10] Bravina, S. L., Morozovsky, N. V., Kulek, J., & Hilczer, B. (1996). *Ukr. Fiz. Zh.*, *41*, 1114.
[11] Bravina, S., Morozovsky, N., Cattan, E., Remiens, D., & Wang, G. (2005). *Integrated Ferroelectrics*, *73*(1), 27.
[12] Bravina, S. L., Morozovsky, N. V., & Strokach, A. A. (1996). Pyroelectricity: Some physical and application aspects In: *Material Science and Material Properties for Infrared Optoelectronics*, Sizov, F. F. (Ed.), SPIE: Bellingham, 3182, 85.
[13] Bravina, S. L., Blonsky, I. V., Morozovsky, N. V., & Salnikov, V. O. (2001). *Ferroelectrics*, *254*, 65.
[14] Poley, L. H., Siqueira, A. P. L., da Silva, M. G., Vargas, H., & Sanches, R. (2004). *Polimeros: Ciencia e Tecnologia*, *14*(1), 8.
[15] Petrov, V. M. (1987). *Izv. Akad. Nauk SSSR, Ser. Fiz.*, *51*, 1763.
[16] Burfoot, J. C. (1967). *Ferroelectrics: An Introduction to the Physical Principles*, Van Nostrand: London.
[17] Jaffe, B., Cook, W. R., & Jaffe, H. (1971). *Piezoelectric Ceramics*, Acad. Press: London.
[18] Iona, F. & Shirane, G. (1962). *Ferroelectric Crystals*, Pergamon Press: London.
[19] Burfoot, J. C. & Taylor, G. W. (1979). *Polar Dielectrics and Their Applications*, Macmillan Press: London.